Construction and Building Materials 220 (2019) 53–63

Contents lists available at ScienceDirect

Construction and Building Materials

journal homepage: www.elsevier.com/locate/conbuildmat

Lateral loading behavior of glulam frame-midply hybrid lateral systems

Wei Zheng [a,*], Weidong Lu [b,*], Weiqing Liu [b], Yue Li [a]

[a] College of Materials Science and Engineering, Nanjing Forestry University, Nanjing 210037, PR China
[b] College of Civil Engineering, Nanjing Tech University, Nanjing 211816, PR China

HIGHLIGHTS

- Load sharing mechanism between the outer frame and infill midply subsystems.
- Hold-down connectors are unnecessary for the infill midply shear walls.
- The post-peak lateral resistance is no less than 70% of load-carrying capacity.
- Midply shear wall is more efficient as an infill than standard wood shear wall.

ARTICLE INFO

Article history:
Received 2 November 2018
Received in revised form 27 May 2019
Accepted 29 May 2019

Keywords:
Wood structures
Frame-midply hybrid
Midply shear walls
Load sharing mechanism
Cyclic loading tests
Lateral loading behavior
High-rise timber buildings

ABSTRACT

This paper presents the results of an experimental study on the lateral loading behavior of glulam frame-midply hybrid lateral systems. Such systems are composed of glulam post-and-beam frames and infill midply shear walls. Reversed cyclic tests of six full-scale glulam frame-midply hybrid systems and two bare post-and-beam frames were conducted. The initial lateral stiffness, lateral load-carrying capacity, ductility and hysteresis characteristics of the hybrid systems were investigated. The load sharing mechanism between the outer frame and the infill midply subsystems was evaluated. Test results show that the installation of the infill midply shear walls can bring great improvements in the lateral resistance and the energy dissipation to the bare post-and-beam frames. The outer post-and-beam frames are basically in elastic range and can effectively restrain the infill midply shear walls from suffering further severe damages. For this reason, the post-peak lateral resistances of the hybrid systems can keep no less than 70% of their own load-carrying capacities within 4.41% drift ratio, and there is no need to install hold-down connectors in the infill midply shear walls. The load-carrying capacity of frame-midply hybrid lateral system is at least 1.5 times that of comparable frame infilled with standard wood-frame shear wall.

1. Introduction

Timber building is well known as the favorable characteristics of environment-friendliness, easy assembly and excellent seismic performance. With the increase of population and the limitation of land resources, conventional low-rise wood-frame constructions become increasingly unsuited in the urban areas, and correspondingly, mid- and high-rise timber buildings have been attracting more and more attention from researchers and engineers. Timber Frame 2000 program initiated by the Building Research Establishment (BRE) of the U.K. was conducted to demonstrate the feasibility and reliability of multistory timber buildings through a series of tests on a full-scale six-story residential building [1,2]. In 1999, a five-year national project was promoted in Japan to develop high-performance timber-based composite members and hybrid structures [3–5]. The SOFIE research project was conducted in Italy to analyze a 7-story building built with cross laminated timber (CLT) panels, considering every single aspect of the building behavior, such as static, fire, acoustic, thermal and, particularly, seismic performance [6–8]. The design methods for mid-rise CLT timber buildings were also discussed, as reported by Fragiacomo et al. [9]. Two notable projects occurred in succession, the CUREE project and the NEESWood project, provided greater understanding, improved analytical modeling, and advances in force- and performance-based seismic design (PBSD) of wood-frame buildings, respectively [10–13].

It is commonly accepted that higher timber buildings often create more demands on the lateral load resisting systems and consequently necessitate improvements in design and construction methods to increase the lateral resistance and ductility of the systems. From a structural point of view, hybridization is an effective

* Corresponding authors.
E-mail addresses: zw@njfu.edu.cn (W. Zheng), wdlu@njtech.edu.cn (W. Lu).

https://doi.org/10.1016/j.conbuildmat.2019.05.182
0950-0618/

method to explore improvements in high-rise timber buildings, since it can take full advantage of the respective benefits of different materials or structural systems. A considerable effort has been reported in the literature for improving the lateral resistance, ductility, and energy dissipation of wooden frames by means of hybridization. Yamada et al. [14] and Miyazawa [15] introduced the effects of three different seismic resistance elements (i.e., plaster walls, wooden braces, and plywood walls) on improving the lateral performance of Japanese conventional wooden frames. The wooden post-and-beam frames hybridized with wood shear walls showed a significant increase in both lateral stiffness and load-carrying capacity under dynamic load conditions. Shim et al. [16] and Park et al. [17] investigated the lateral performance of the glulam frame-shearwall hybrid system which is composed of timber post-and-beam frame and infill wood-frame shear wall. He et al. [18] evaluated the lateral performance of timber-steel hybrid shear wall system under cyclic loading condition. The test results revealed that stronger infill led to higher lateral resistance and energy dissipation of timber-steel hybrid shear wall system.

Midply shear wall developed by FPInnovations [19] has been shown to provide two to three times as much lateral resistance as comparable standard wood shear wall, as reported in Varoglu et al. [20–22]. Apparently, this novel shear wall can be considered as an improved infill in the post-and-beam frame, forming frame-midply hybrid lateral system to resist lateral loads. Although the lateral performance of glulam frame infilled with standard wood-frame shear wall has been investigated by some researchers, it is necessary to investigate the behavior of frame-midply hybrid system under earthquake loads, particularly the load sharing mechanism between the outer post-and-beam frame and the infill midply shear wall. This paper presents the cyclic test results of six full-scale frame-midply hybrid systems and two bare post-and-beam frames, aiming to provide technical support for the application of this hybrid system in mid- and high-rise timber buildings.

2. Experimental program

2.1. Material

The materials adopted in this experimental study are as follows:

1. Canadian Douglas fir glued-laminated (glulam) timber was used to fabricate the columns and beams for the post-and-beam frames. The elastic modulus of the glulam members was about 12000 MPa, and the moisture content was 15% on average.
2. Bolts and anchor bolts in 8.8-grade (equivalent to ASTM A325 bolts), conforming to Chinese Standard GB/T 1231-2006 [23], were used as fasteners in the specimens. The maximum tensile stress of all the bolts was no less than 800 MPa, and the yield stress was no less than 640 MPa.
3. Mild carbon Q235B steel plates of 10 mm in thickness, conforming to Chinese Standard GB 50017-2017 [24], was welded to fabricate the T-shape steel connectors for the wood-steel-wood bolted connections in the glulam frames. The yield stress of the steel plates was 235 MPa.
4. Performance rated 19/32 (Engineered Wood Association panel grade) oriented strand boards (OSB), 1220 × 2440 mm in panel size, 12.5 mm and 15.5 mm in thickness, were used as mid-sheathing panel for the infill midply shear walls.
5. Canadian No. 2 spruce-pine-fir (SPF) 38 × 89 mm lumbers, with an average moisture content of 12%, were used as framing members (i.e., studs, top plates, and bottom plates) of the infill midply shear walls.
6. Galvanized spiral nails of 3.6 mm in diameter and 82 mm in length were adopted as framing-sheathing-framing fasteners in the infills. The nails were driven with a nail gun. The bending behavior of the nails was tested according to ASTM F1575 [25], as reported in Zheng et al. [26]. The nominal fastener yield strength was 706.7 MPa.

2.2. Specimen design

Six frame-midply hybrid systems (“FMW” series) were designed and tested under cyclic loading conditions to check the effect of the following variables: (1) size of infill midply shear wall; (2) nail spacing and mid-sheathing panel thickness in infill midply shear wall; (3) application of vertical load. Two bare post-and-beam frames (“F” series) with different aspect ratio were tested similarly for comparison. Table 1 shows the detail information of the specimens.

Fig. 1 shows a typical glulam frame-midply hybrid lateral system in detail. The outer glulam frame and the infill midply shear wall served as subsystems in the hybrid system. In the infill midply shear wall, one ply of OSB sheathing panels was placed at the center of the wall between a series of pairs of studs and plates oriented in 90° rotated position relative to those in standard shear walls, as detailed in Varoglu et al. [21]. No. 2 SPF 38 × 89 mm lumbers were used as studs and plates. The studs were spaced 406 mm on center. The OSB panels were sandwiched between pairs of studs and plates with 82-mm-long × 3.6-mm-diameter spiral nails at 100 or 150 mm spacing along the panel edges and at 200 or 300 mm spacing along the intermediate studs. A 12-mm gap was reserved between the bottom edge of the mid-sheathing panel and the lower edge of the bottom plates, and the same relationship held for the top edge of the mid-panel and the upper edge of the top plates. Therefore, the rotation of the mid-sheathing panels would not be restricted during the test.

The outer glulam frame was assembled with two square columns and a rectangular beam. The sectional dimensions of the column and the beam were 200 mm × 200 mm and 150 mm × 260 mm, respectively. Wood-steel-wood bolted connections were adopted in the outer glulam frame, as shown in Fig. 1(c) and (d). A height of 2.72 mm and two lengths of 3.25 mm and 3.86 mm were designed for the outer frames, according to the sizes of their infill midply shear walls. The bare post-and-beam frames (specimens F1 and F2) for comparison were constructed identically.

In order to make the two subsystems working as a whole, four pairs of M12 bolts, with two in a row and row spacing of 600 mm, were used to connect each pair of end studs of the infill midply shear wall to the frame column, and similarly, several pairs of bolts with row spacing of 406 mm connected the top plates to the frame beam. There were no hold-down connectors installed in the infill midply shear walls.

2.3. Test setup

Fig. 2 shows the test setup for the cyclic tests of the specimens. A hydraulic actuator capable of 250 kN was situated in line with the frame beam through a specially-made steel connector to exert racking forces on the specimen during a test. The stroke of the actuator is 500 mm. The testing started at the midpoint of the stroke so that the specimens could be pushed and pulled 250 mm either way in a reverse-cyclic test. The frame column base was rigidly mounted (by four M18 bolts) on a steel ground beam which was securely fixed on the structural floor. The bottom plates of the infill midply shear walls were fixed on the steel anchor beam with a series of pairs of M12 bolts at 406 mm row spacing. A constant vertical load of 200 kN was designed for specimens FMW3 and FMW6, with 100 kN applied on each column via stretching steel strands with two hydraulic central-hole jacks. The vertical load represented the weight of about three storeys above the hybrid system. Additionally, out-of-plane stability of the specimens was ensured via several steel rollers installed on the lateral supports.

Table 1
Test matrix.

Specimen number	Length × height (m × m)	Size of infill midply (m × m)	Mid-sheathing thickness (mm)	Nail spacing (mm) edge/interior	Vertical load (kN)
FMW1	3.25 × 2.72	3.05 × 2.46	12.5	100/200	–
FMW2	3.86 × 2.72	3.66 × 2.46	12.5	100/200	–
FMW3	3.86 × 2.72	3.66 × 2.46	12.5	100/200	200
FMW4	3.86 × 2.72	3.66 × 2.46	15.5	100/200	–
FMW5	3.86 × 2.72	3.66 × 2.46	15.5	150/300	–
FMW6	3.86 × 2.72	3.66 × 2.46	15.5	100/200	200
F1	3.25 × 2.72	–	–	–	–
F2	3.86 × 2.72	–	–	–	–

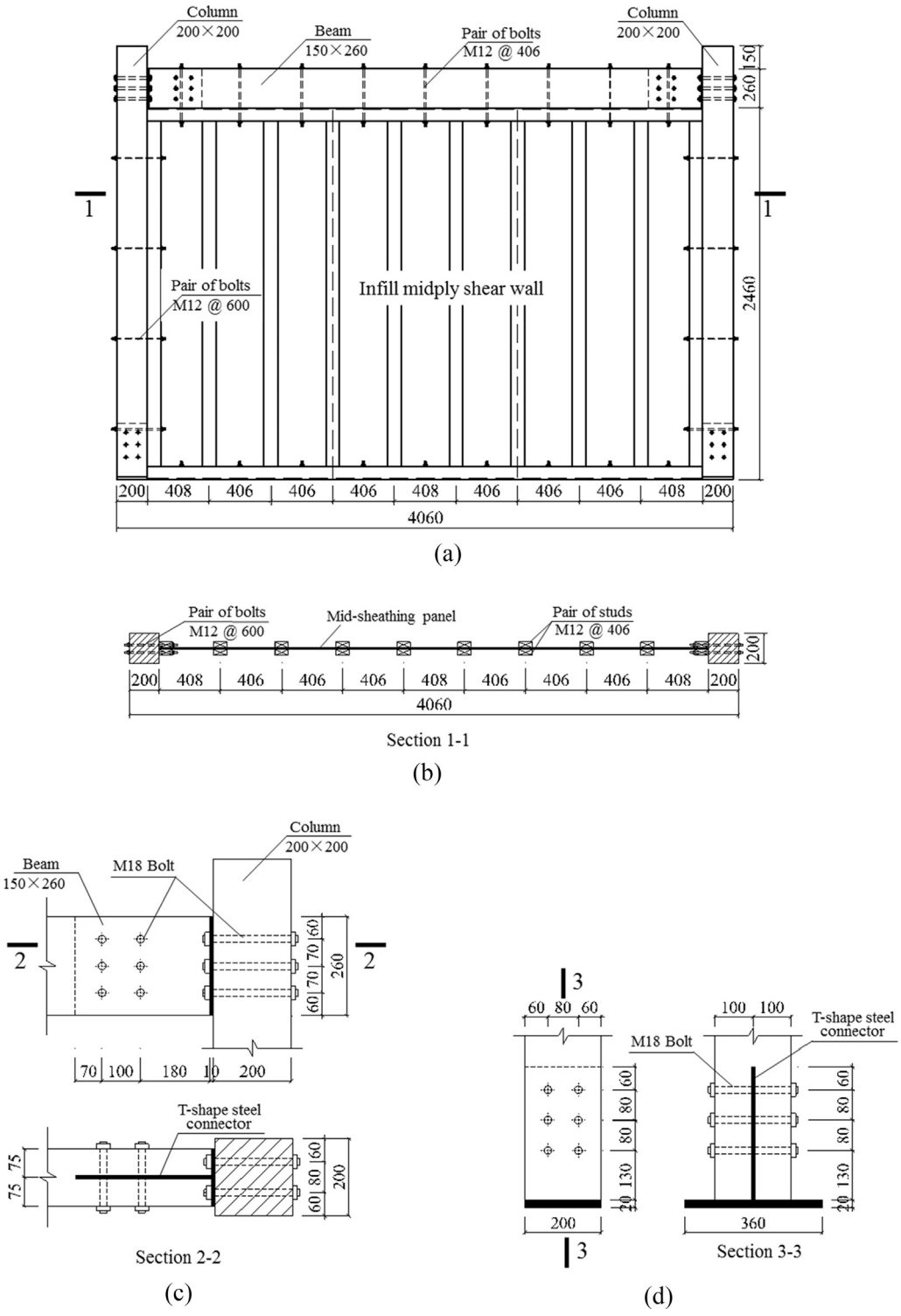

Fig. 1. Configurations of a typical glulam frame-midply hybrid lateral system: (a) overview; (b) top view section; (c) beam-to-column connection; (d) column base connection (all dimensions are in mm).

2.4. Test procedures

The reversed cyclic loading protocol in this research was determined according to Chinese Standard JGJ 101-96 [27] (Specification of test methods for earthquake resistant building) and the ISO Standard ISO-16670 [28] (Timber structures—joint made with mechanical fastener—quasi-static reversed-cyclic test method). The protocol employed a displacement control scheme consisting of two displacement patterns, as follows: (1) single reversed cycle at displacement of 2.5, 5.0, 7.5, and 10% of $\triangle_m$ (the ultimate displacement); (2) phases containing three reversed cycles of equal amplitude, at displacement of 20, 40, 60, 80, 100, and 120% of $\triangle_m$. For the bare post-and-beam frames, in consideration of their high deformability, additional three reversed cycles of equal amplitude at displacement of 160, and 120% of $\triangle_m$ were added following the second displacement pattern. The ultimate displacement $\triangle_m$ was set as 100 mm according to the test results of midply shear walls reported in Varoglu et al. [21]. The detailed loading protocols were shown in Fig. 3.

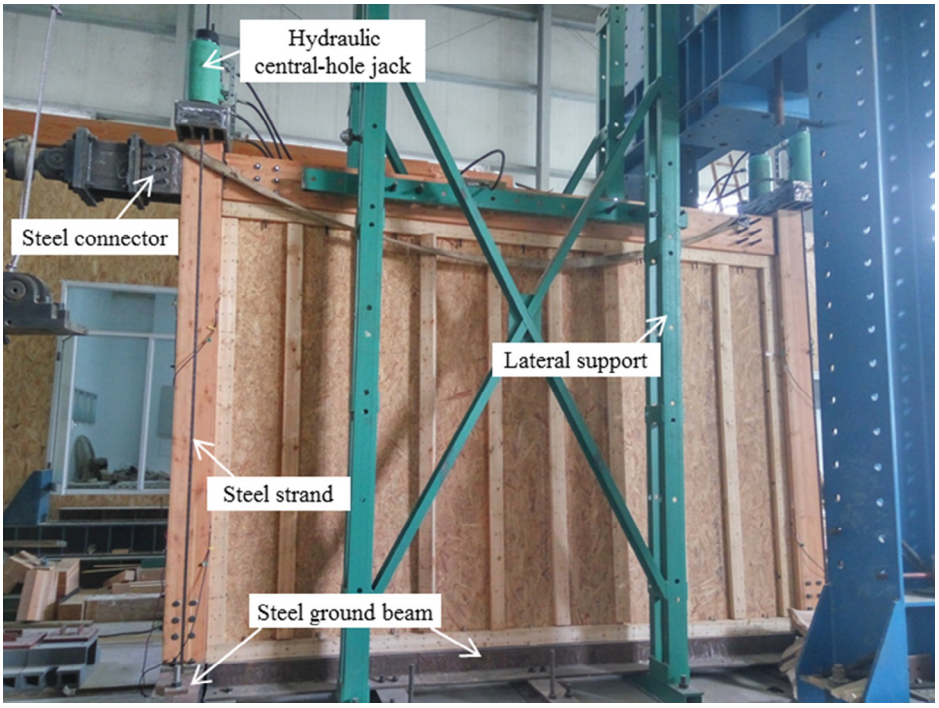

Fig. 2. Test setup.

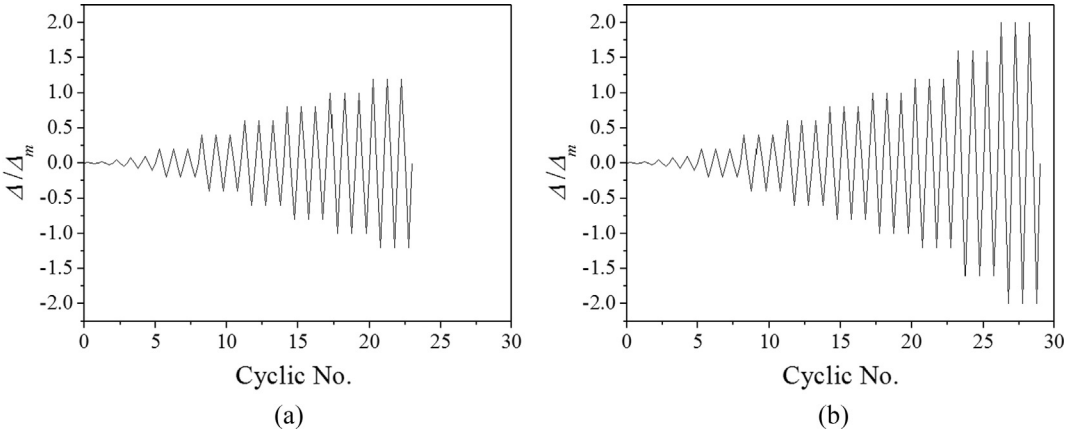

Fig. 3. Test protocols for (a) frame-midply hybrid systems; (b) bare post-and-beam frames.

2.5. Data acquisition

The lateral deformation of each specimen was recorded by a LVDT (linear variable displacement transducer) situated in line with the central axis of the frame beams. For each frame-midply hybrid system, 16 strain gauges were used to record the strain of the outer frame columns, as shown in Fig. 4. As the lateral force applied on frame-midply hybrid system was simultaneously resisted by the outer post-and-beam frame and the infill midply shear wall, the following calculation procedure proposed by He et al. [18] was employed to evaluate the load sharing behavior between the two subsystems.

For each frame-midply hybrid system, the applied shear force P was separated into two parts: the shear force carried by the outer post-and-beam frame (P_f) and that carried by the infill midply shear wall (P_w). P_f could be calculated as the summation of the shear force in the left column (P_l) and that in the right column (P_r). Strain gauges S1 to S8 located at the 1.2-m length of the left column were used to calculate P_l, and similarly, strain gauges S9 to S16 located at the 1.2-m length of the right column were used to calculate P_r. The 1.2-m portion of column was close to the inflection point and was always in elastic range during the test. Since the shear force equals to the changing rate of bending moment, P_l and P_r can be obtained according to Eq. (1):

$$P_{lorr} = \frac{M_t + M_b}{L} = \frac{(\varepsilon_{tmax} + \varepsilon_{bmax} - \varepsilon_{tmin} - \varepsilon_{bmax})EW}{2L} \quad (1)$$

in which, M_t (M_b) represent the bending moment at the top (bottom) section of the 1.2-m-length frame column; L is equal to 1.2 m; $\varepsilon_{t\,max}$ ($\varepsilon_{t\,min}$) is the maximum (minimum) strain at the top section of the 1.2-m-length column, and equals to the average reading of the two strain gauges on one (another) side of the top section; $\varepsilon_{b\,max}$ ($\varepsilon_{b\,min}$) is the maximum (minimum) strain at the bottom section of the 1.2-m-length column, and equals to the average reading of the two strain gauges on one (another) side of the bottom section; E and W represent the elastic modulus of glulam timber and the section modulus of the frame column, respectively. Finally, the shear force in the infill midply shear wall (P_w) can be calculated by using Eq. (2):

$$P_w = P - (P_l + P_r) \quad (2)$$

3. Results and discussion

3.1. Failure modes

For the bare post-and-beam frames, there was no significant damage observed during the whole period of the test, except for slightly cleavage crack developed along the grain at the bottom of the frame column when the lateral displacement reached

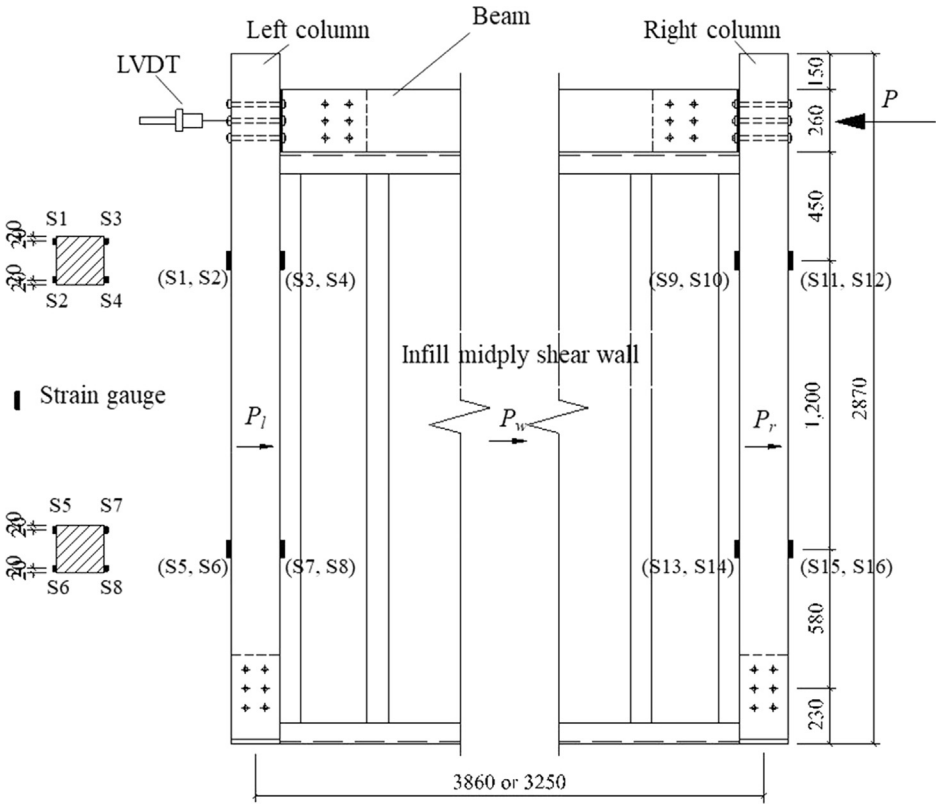

Fig. 4. Arrangements of LVDT and strain gauges.

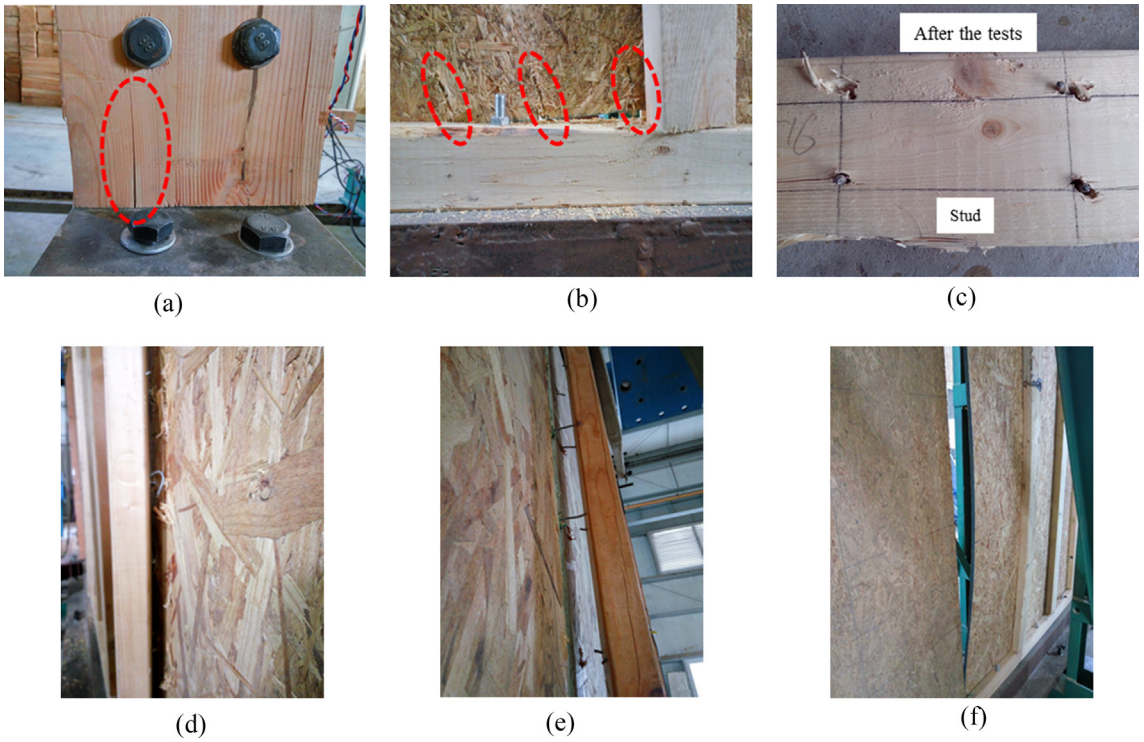

Fig. 5. Failure modes: (a) cleavage crack at the bottom of the frame column; (b) nail tear out failure; (c) nail fatigue fracture; (d) nail withdrawal; (e) detachment of the intermediate studs at the panel joints; (f) buckling of the mid-sheathing panel.

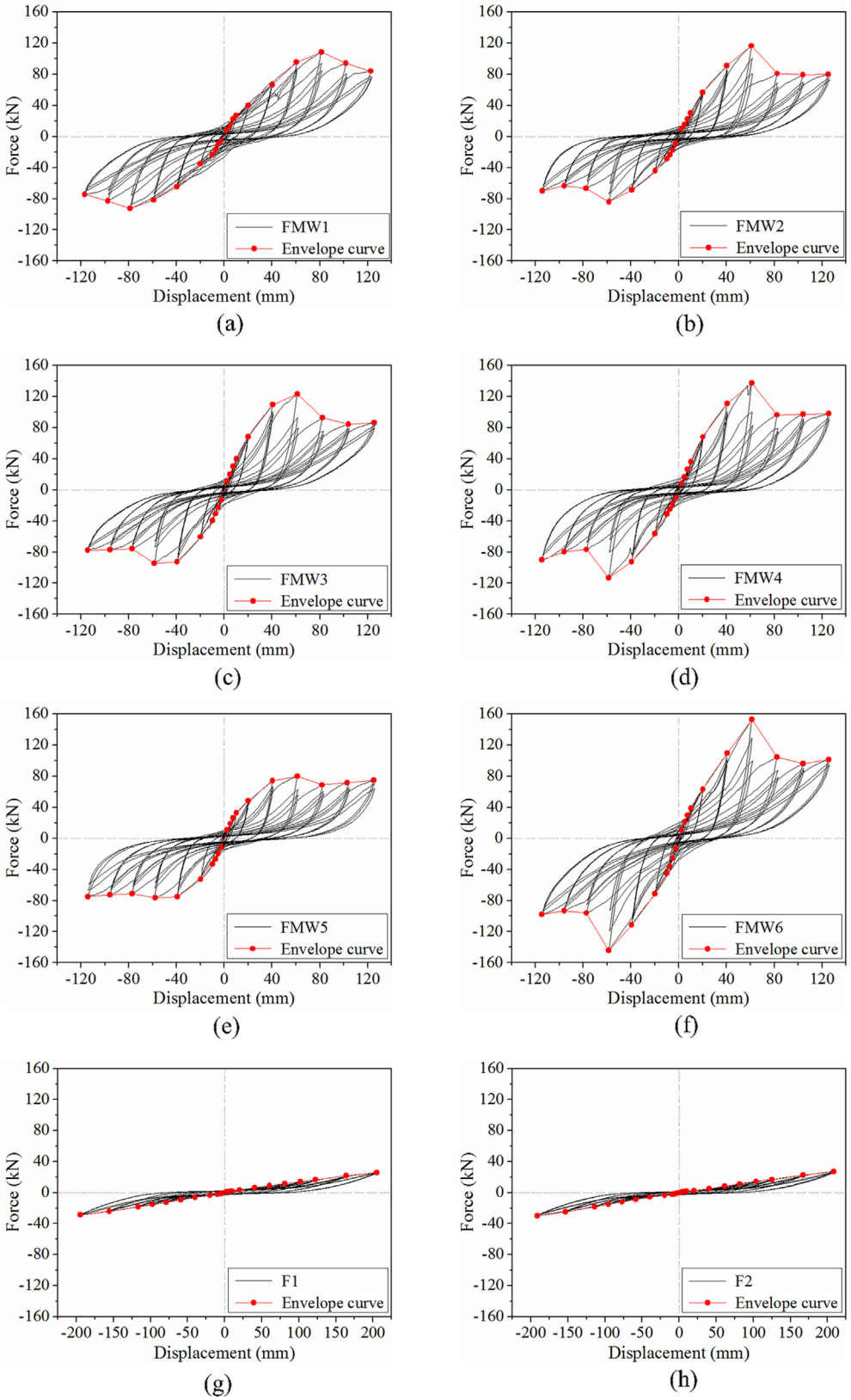

Fig. 6. Hysteretic loops of specimen: (a) FMW1; (b) FMW2; (c) FMW3; (d) FMW4; (e) FMW5; (f) FMW6; (g) F1; (h) F2.

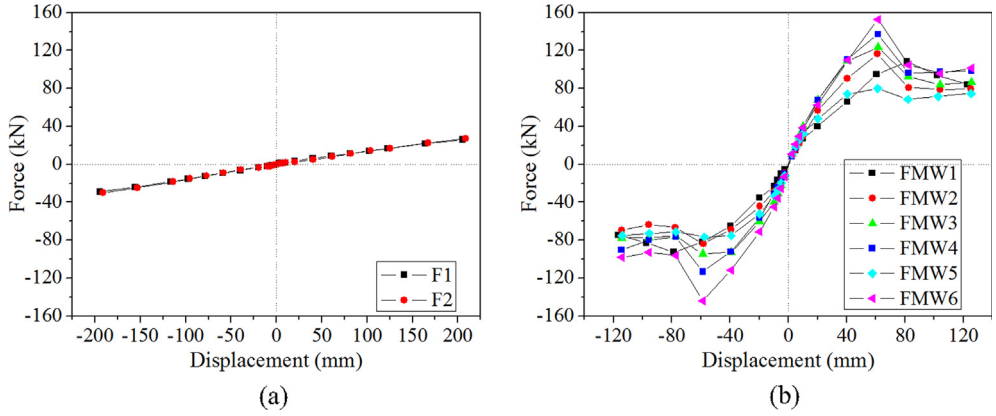

Fig. 7. First envelope curves of: (a) the bare post-and-beam frames; (b) the frame-midply hybrid systems.

Table 2
Summary of test results.

Specimen number	P_{peak} (kN)	V_{peak} (kN/m)	Δ_{peak} (mm)	K_e [(kN/mm)/m]	P_{yield} (kN)	Δ_{yield} (mm)	Δ_u (mm)	D
FMW1	100.57	30.94	80	0.56	88.62	48.21	117.33	2.43
FMW2	100.15	25.95	59.7	0.71	84.63	30.82	75.98	2.47
FMW3	108.9	28.21	60.1	1.0	95.8	25.12	77.62	3.09
FMW4	125.27	32.45	60.1	0.82	107.26	33.73	72.86	2.16
FMW5	78.36	20.3	59.48	0.79	66.61	21.84	119.71	5.48
FMW6	148.33	38.43	60.07	0.91	124.77	35.99	72.33	2.01

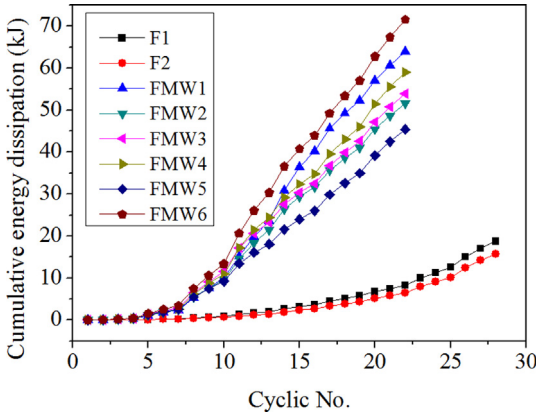

Fig. 8. Cumulative energy dissipation.

120 mm, as shown in Fig. 5(a). The crack did not spread through the bolt hole, and therefore it had little effect on the behavior of the wood-steel-wood bolted connection. Moreover, there was no bending deformation observed on the bolts after splitting the joint connections.

For the frame-midply hybrid systems, the failure modes were quite similar and mainly occurred in the infill midply shear walls. Initially, nail tear out failures were observed on the edge of the mid-sheathing panel, as shown in Fig. 5(b). The specimens reached their ultimate bearing capacity state at the lateral displacement of about 60 mm (2.21% drift ratio), along with lots of nail fatigue fracture failures and few of nail withdrawal failures appeared, as shown in Fig. 5(c) and (d), respectively. The nail fatigue fracture was mainly due to the reversed cyclic slippage between the mid-sheathing panel and the SPF studs, which causes the reduplicative bending of nail. At the end of the tests, it was precisely because of these mentioned nail connection failures, the pair of studs at the panel joint detached from the mid-sheathing panel, and then furtherly leading to the buckling of mid-sheathing panel, as shown in Fig. 5(e) and (f). The bolt connections between the outer frame and the infill subsystems kept in good condition during the whole period of the test, and little relative slip between the subsystems was observed. Moreover, there was hardly any uplift of the end studs observed in the infill midply shear walls. Hence, it can be concluded that the installation of hold-down connectors is unnecessary for the infill midply shear walls.

3.2. Lateral load capacity

Fig. 6 shows the hysteretic loops of the test specimens. It can be observed that the hysteretic loops of the frame-midply hybrid systems (specimens FMW1 ~ FMW6) are much plumper than those of the bare post-and-beam frames (specimens F1 and F2). Fig. 7 shows the comparison of the first envelope curves of the test specimens. The first envelope curves of the two bare post-and-beam

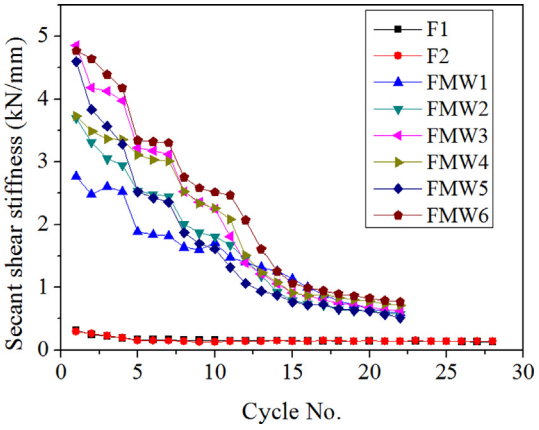

Fig. 9. Stiffness degradation.

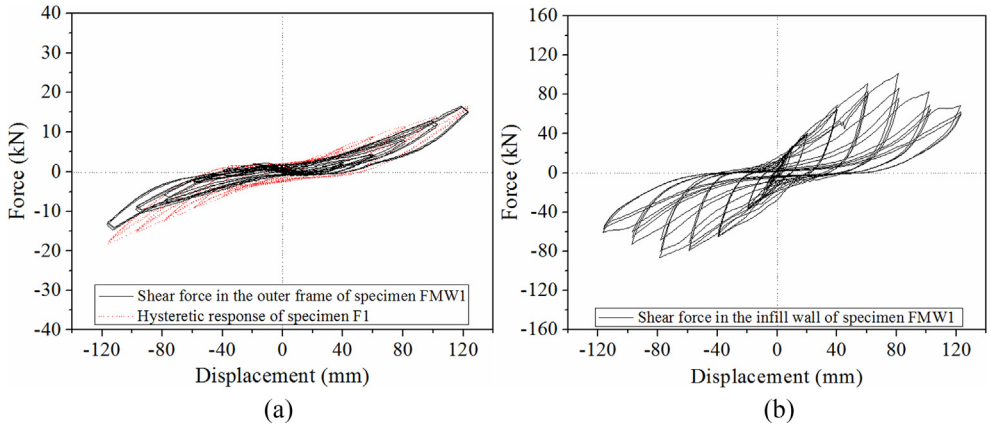

Fig. 10. Lateral load sharing in the subsystems of specimen FMW1: (a) shear force in the outer post-and-beam frame; (b) shear force in the infill midply shear wall.

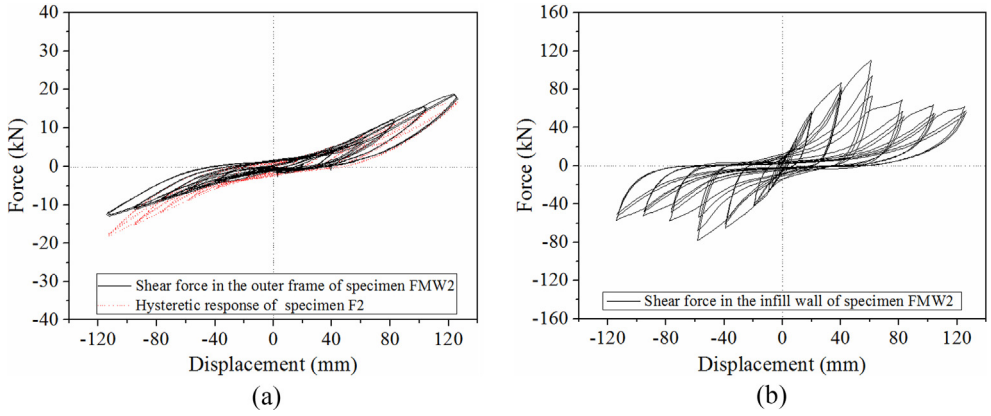

Fig. 11. Lateral load sharing in the subsystems of specimen FMW2: (a) shear force in the outer post-and-beam frame; (b) shear force in the infill midply shear wall.

frames are almost overlapping and exhibit linear elastic features. These phenomena were primarily determined by the moment-rotation behavior of the beam-to-column connections and the column base connections in the frames. By contrast, obvious nonlinearities are observed on the first envelope curves of the frame-midply hybrid systems, mainly resulting from the nail connection failures in the infill midply shear walls. By comparing the envelope curves in Fig. 7(a) and (b), it can be found that both the lateral load capacity and the initial stiffness of specimen FMW1 and FMW2 are much higher than those of the bare post-and-beam specimen F1 and F2, respectively, although they have identical overall sizes. Hence, the installation of infill midply shear wall can significantly increase the lateral resistance of bare post-and-beam frame.

The lateral load capacity parameters for the frame-midply hybrid system can be calculated from their first envelope curves according to ASTM E2126 [29]. The definitions and calculations of the parameters are listed as follows:

1. P_{peak} (kN): maximum shear load of the frame-midply hybrid system;
2. V_{peak} (kN/m): average shear strength of the frame-midply hybrid system, which means the lateral load capacity of the unit length of the hybrid system. $V_{peak} = P_{peak}/L$, where L is the length of the hybrid system;
3. Δ_{peak} (mm): displacement corresponding to maximum shear load;
4. K_e [(kN/mm]/m]: average initial stiffness of the unit length of the frame-midply hybrid system. $K_e = 0.4P_{peak}/(\Delta_{0.4Ppeak}\ L)$, where $\Delta_{0.4Ppeak}$ is the displacement at 40% of maximum shear load;
5. P_{yield} (kN): yield load of the specimen, which was determined by using the EEEP (equivalent energy elastic-plastic) curve, according to ASTM E 2126 [29];
6. Δ_{yield} (mm): displacement corresponding to yield load, $\Delta_{yield} = P_{yield}/K_e$;
7. Δ_u (mm): ultimate displacement of the frame-midply hybrid system, which is the displacement at the load degraded to the value equal to 80%P_{peak};
8. D: cyclic ductility factor, $D = \Delta_u/\Delta_{yield}$.

Push-pull average values of the above-mentioned parameters for the hybrid systems, as given in Table 2, were used to evaluate their lateral loading behavior.

As shown in Table 2, the shear strength and the initial stiffness of specimen FMW4 were equal to 32.45 kN/m and 0.82 (kN/mm)/m, respectively, which were 59.85% and 3.8% greater than those of specimen FMW5, respectively, and 25.05% and 15.49% greater than those of specimen FMW2, respectively. It should be noted that the shear strength of specimen FMW2 was at least 1.5 times that of the comparable frame infilled with standard wood-frame shear wall as reported by Park et al. [17] and Xiong and Liu [30]. In the research of Park et al., the shear strength of the glulam frame infilled with standard wood-frame shear wall (Specimen NSW) was 18.6 kN/m. The sectional dimensions of the glulam column and beam were 150 mm × 150 mm and 150 mm × 240 mm, respectively. The infill standard wood shear wall (3.48 m × 2.45 m in size) was sheathed on both sides with 11.1-mm-thick OSB panels at 150/200 mm nail spacing. Xiong and Liu [30] obtained an identical result of shear strength (Specimen CFW1) which was equal to 18.7 kN/m. The infill standard wood

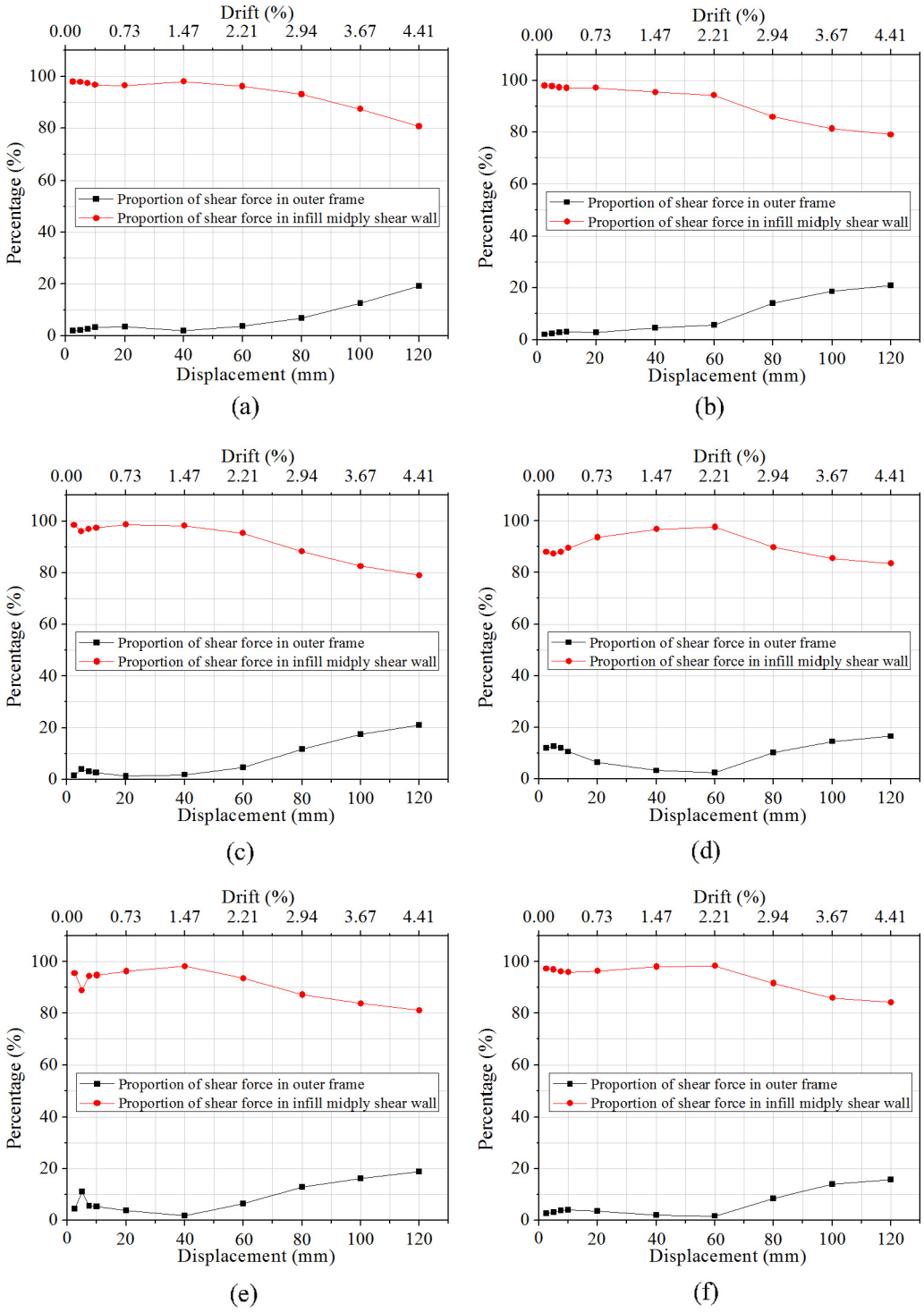

Fig. 12. Proportion of shear force resisted by the subsystems in specimen: (a) FMW1; (b) FMW2; (c) FMW3; (d) FMW4; (e) FMW5; (g) FMW6.

shear wall of specimen CFW1 was 3.83 m × 2.46 m in plan size, and the sectional dimension of the glulam frame is 150 mm × 150 mm for the column and 150 mm × 240 mm for the beam. It also should be noted that if the infill standard wood-frame shear walls were sheathed on single side, the shear strength of the hybrid systems would be even lower.

The shear strength of specimens FMW3 and FMW6 (subjected to 200 kN vertical load) were equal to 28.21 kN/m and 38.43 kN/m, respectively, which were 8.74% and 18.41% greater than those of specimens FMW2 and FMW4 (without vertical load), respectively. Besides, the initial stiffness of specimens FMW3 and FMW6 were 41.03% and 11.18% greater than those of specimens FMW2 and FMW4, respectively. Hence, it can be concluded that the application of vertical load also can effectively improve the lateral resistance of frame-midply hybrid system.

The displacement ductility factor (D) is introduced to evaluate the ductility performance of the frame-midply hybrid systems. As presented in Table 2, the values of D range from 2.01 to 5.48. Among them, the displacement ductility factor of specimen FMW5 with 150/300 mm nail spacing was the highest, and those

of the other specimens with 100/200 mm nail spacing were quite close and much lower than the former. However, the hybrid system with a nail spacing smaller than 150/300 mm is preferable when used in mid- and high- rise timber buildings, due to the high demands on their lateral stiffness and strength.

It also should be noted that the post-peak lateral resistance of each frame-midply hybrid system maintained no less than 70% of its own load-carrying capacity (P_{peak}), according with the plateau region in the descending phase of the first envelope curve, as shown in Fig. 7(b).

3.3. Hysteretic characteristics

Since the energy-dissipating capacity is beneficial for a building to prevent from collapsing, energy dissipation is generally regarded as an important parameter for evaluating the lateral performance of a structure or system. Under cyclic loading conditions, energy dissipation of frame-midply shear wall hybrid systems mainly derived from the internal frictions of components, the failures of the nail connections, and some unrecoverable deformations. The energy dissipation of the specimens can be measured by calculating the area of the hysteretic loops (as presented in Fig. 6).

Fig. 8 shows the cumulative energy dissipation for the two bare post-and-beam frames and six frame-midply hybrid systems. It can be found that the cumulative energy dissipation in the bare post-and-beam frames was far less than that in the frame-midply hybrid systems, indicating that the energy-dissipating capacity of the hybrid systems was mainly provided by their infill midply subsystems. The hysteretic energy dissipation for each frame-midply hybrid system was extremely small during the first seven loading cycles corresponding to the drift ratio of 0.74%. In this stage, the hybrid systems worked approximately elastically without any damages. After that, the energy dissipation increased rapidly, due to the continuous failures of the nail connections in the infill midply subsystems. Among all the six frame-midply hybrid systems, specimen FMW6 (subjected to 200 kN vertical load) dissipated the most energy, and specimen FMW5 (with 150/300 mm nail spacing) exhibited the lowest energy dissipation. Thus, it can be concluded that nail spacing and upper vertical load were the two most sensitive factors affecting the energy-dissipating capacity of frame-midply hybrid systems.

Stiffness degradation is another important parameter in the evaluation of the lateral performance of a structure or system, which can be determined using the secant shear stiffness of each loading cycle calculated as Eq. (3) [27]:

$$K_i = \frac{|F_i^+| + |F_i^-|}{|\Delta_i^+| + |\Delta_i^-|} \tag{3}$$

in which, K_i is the secant shear stiffness of the ith cycle, kN/mm; F_i is the maximum load in the ith cycle, kN; and Δ_i is the displacement corresponding to the maximum load F_i, mm.

Fig. 9 shows the stiffness degradation results of all the specimens. It can be found that the secant shear stiffness of the two bare post-and-beam frames were exactly similar and roughly kept in a constant value of 0.15 kN/mm, according with their elastic load-displacement behaviors. By contrast, all the six frame-midply hybrid system exhibited obvious stiffness degradation characteristics, which occurred mainly within the first fourteen cycles (within 2.94% drift ratio). After that, the speed of stiffness degradation slowed. The secant shear stiffness of the hybrid systems subjected to 200 kN vertical load (specimens FMW3 and FMW6) were higher than those of the identical specimens without the vertical load throughout the test.

3.4. Load sharing mechanism between frame and midply

For each frame-midply hybrid lateral system, the shear forces resisted by the two subsystems were calculated according to Eqs. (1) and (2). For instance, the calculation results of specimens FMW1 and FMW2 are shown in Figs. 10 and 11, respectively. It can be found that the outer post-and-beam frame and the infill midply shear wall roughly maintained their own lateral loading behaviors in the hybrid systems. Especially, the shear force-displacement curves of the outer frames in specimens FMW1 and FMW2 agreed well with the hysteretic responses of the bare frames F1 and F2, respectively, as shown in Figs. 10(a) and 11(a). Based on the calculation results, the proportion of the shear force resisted by each subsystem was obtained and shown in Fig. 12. These percentage values were calculated with the method of dividing the shear forces in each subsystem by the shear force applied to the structure.

All the six frame-midply hybrid systems exhibited similar load sharing mechanism. Before the hybrid systems achieved their peak strength (within 2.21% drift ratio), the infill midply subsystems carried almost 90% of the applied load, due to the huge gap between the initial lateral stiffness of the two subsystems. As testing proceeded (above 2.21% drift ratio), more and more nail connection failures occurred in the infill midply subsystems, resulting in the decline of the infills' lateral load resistance. However, until the end of the tests, the percentage values of the shear force in the infill midply subsystems still kept more than 80 percent, even though the studs at the panel joint detached (see Fig. 5(e)) from the infill midply shear walls at 2.94% drift ratio. This was mainly due to the fact that the infill midply subsystems were effectively restrained by the outer frame subsystems from suffering further severe damages, such as the buckling failure or the tension failure at the end stud, as reported by Varoglu et al. [21]. During the whole period of the tests, the proportions of the shear force resisted by the outer frame subsystems kept increasing slowly. However, the values did not exceeded 20 percentages within 4.41% drift ratio, indicating that the lateral load resistance of the outer frame subsystems could not be fully employed in frame–midply hybrid systems.

4. Conclusions

This paper presents the cyclic test results of six frame-midply hybrid lateral systems and two bare post-and-beam frames. The lateral load capacities and the hysteretic characteristics of the frame-midply hybrid lateral systems were investigated. The load sharing mechanism between the outer frame and the infill midply subsystems was discussed. The test results show that the installation of the infill midply shear walls bring great improvements in the lateral resistance and the energy dissipation of bare post-and-beam frames. The lateral load-carrying capacity of the frame-midply hybrid lateral system tested is at least 1.5 times that reported for comparable frame infilled with standard wood-frame shear wall.

The detachment of the stud at the panel joint in infill midply shear walls, resulting from the failures of nail connections, is the final failure mode of frame-midply hybrid lateral systems under cyclic lateral loading. The lateral load resistances and the hysteretic characteristics of the hybrid systems are dependent mainly on their infill midply subsystem, and are correspondingly affected by the infill midply's variables in terms of nail spacing, mid-sheathing thickness and wall size. The application of vertical load can increase the initial lateral stiffness, the strength and the energy dissipation of the hybrid systems. Rapid stiffness degradation of the hybrid systems develops mainly within 2.94% drift ratio, due to the damage accumulated in the infill midply shear walls.

In terms of the load sharing effect between the outer frame and the infill midply subsystems, the infill midply shear walls are very effective, absorbing more than 80% of the lateral load. The outer frames are basically in elastic range, but can effectively restrain the infill midply shear walls from suffering further severe damages in the case of large deformation. For this reason, there is no need to install hold-down connectors in the infill midply shear walls. Moreover, the post-peak lateral resistances of the hybrid systems can keep no less than 70% of their own load-carrying capacities within 4.41% drift ratio, contributing to prevent them from collapsing.

This study aims to provide an excellent lateral force resisting system for mid- and high-rise timber buildings, and the presented results may provide technical support for the development of guidelines for using such hybrid system in practical engineering.

Declaration of Competing Interest

The authors declare that there is no conflict of interest.

Acknowledgements

The authors gratefully acknowledge National Natural Science Foundation of China (Grant No. 51808293) and Natural Science Foundation of Jiangsu Province, China (Grant No. BK20180778).

References

[1] T. Lennon, M. Bullock, V. Enjily, The fire resistance of medium-rise timber frame buildings, Proc. 6th World Con. on Timber Engineering, 2000.
[2] B.R. Ellis, A.J. Bougard, Dynamic testing and stiffness evaluation of a six-storey timber framed building during construction, Eng. Struct. 23 (10) (2001) 1232–1242.
[3] I. Sakamoto, N. Kawai, H. Okada, N. Yamaguchi, H. Isoda, S. Yusa, Final report of a research and development project on timber-based hybrid building structures, Proc. 8th World Con. on Timber Engineering, Finnish Association of Civil Engineers, 2004.
[4] M. Yamaguchi, N. Kawai, T. Murakami, N. Shibata, Y. Namiki, Constructions and researches after the project of developing hybrid timber buildings, Proc. 8th World Con. on Timber Engineering, Finnish Association of Civil Engineers, 2004.
[5] M. Koshihara, H. Isoda, The design and installation of a five-story new timber building in Japan, in: Summary of Technical Papers of the Annual Meeting of the Architectural Institute of Japan, Architectural Institute of Japan, Tokyo, Japan, 2005, pp. 201–206.
[6] A. Ceccotti, New technologies for construction of medium-rise buildings in seismic regions: the XLAM case, Struct. Eng. Int. 18 (2) (2008) 156–165.
[7] B. Dujic, K. Strus, R. Zarnic, A. Ceccotti, Prediction of dynamic response of a 7-storey massive X-lam wooden building tested on a shaking table, Proc. 11th World Conf. on Timber Engineering, 2010.
[8] G. Rinaldin, M. Fragiacomo, Non-linear simulation of shaking-table tests on 3- and 7-storey X-Lam timber buildings, Eng. Struct. 113 (2016) 133–148.
[9] M. Fragiacomo, B. Dujic, I. Sustersic, Elastic and ductile design of multi-storey crosslam massive wooden buildings under seismic actions, Eng. Struct. 33 (11) (2011) 3043–3053.
[10] J.W. van de Lindt, S. Pei, S.E. Pryor, H. Shimizu, H. Isoda, Experimental seismic response of a full-scale six-story light-frame wood building, J. Struct. Eng. 136 (10) (2010) 1262–1272.
[11] W. Pang, D.V. Rosowsky, S. Pei, J.W. van de Lindt, Simplified direct displacement design of six-story woodframe building and pretest seismic performance assessment, J. Struct. Eng. 136 (7) (2010) 813–825.
[12] J.W. van de Lindt, S.E. Pryor, S. Pei, Shake table testing of a full-scale seven-story steel-wood apartment building, Eng. Struct. 33 (3) (2011) 757–766.
[13] J.W. van de Lindt, D.V. Rosowsky, W. Pang, S. Pei, Performance-based seismic design of midrise woodframe buildings, J. Struct. Eng. 139 (8) (2013) 1294–1302.
[14] M. Yamada, Y. Suzuki, M. Gotoum, Seismic performance evaluation of Japanese wooden frames, Proc. 13th World Con. on Earthquake Engineering, 2004.
[15] K. Miyazawa, Full-scale shaking table tests of two-story wooden dwelling houses in Japan, Proc. 10th World Con. on Timber Engineering, 2008.
[16] K.B. Shim, K.H. Hwang, J.S. Park, Lateral load resistance of hybrid wall, Proc. 11th World Con. on Timber Engineering, 2010.
[17] M.J. Park, K.H. Hwang, J.S. Park, K.B. Shim, Shear performance of hybrid post and beam wall system with structural insulation panel infill, Proc. 11th World Con. on Earthquake Engineering, 2010.
[18] M. He, Z. Li, F. Lam, R. Ma, Z. Ma, Experimental investigation on lateral performance of timber-steel hybrid shear wall systems, J. Struct. Eng. 140 (6) (2014). 04014029-1-4014029-12.
[19] E. Varoglu, S. Stiemer, Wood wall structure, United State Patent No. 5782054, 1998.
[20] E. Karacabeyli, S. Stiemer, C. Ni, MIDPLY shearwall system, Structures 2001: A Structural Engineering Odyssey, (2001), pp. 1–17.
[21] E. Varoglu, E. Karacabeyli, S. Stiemer, C. Ni, Midply wood shear wall system: concept and performance in static and cyclic testing, J. Struct. Eng. 132 (9) (2006) 1417–1425.
[22] E. Varoglu, E. Karacabeyli, S. Stiemer, C. Ni, M. Buitelaar, D. Lungu, Midply wood shear wall system: performance in dynamic testing, J. Struct. Eng. 133 (7) (2007) 1035–1042.
[23] GB/T 1231-2006, Specifications of High Strength Bolts with Large Hexagon Head, Large Hexagon Nuts, Plain Washers for Steel Structures, National Standards of the People's Republic of China, Beijing, China, 2006.
[24] GB 50017-2017, Code for Design of Steel Structures, National Standards of the People's Republic of China, Beijing, China, 2017.
[25] ASTM: F1575-03, Standard Test Methods for Determining Bending Yield Moment of Nails, ASTM Standards, West Conshohocken, PA, USA, 2003.
[26] W. Zheng, W. Lu, W. Liu, L. Wang, Z. Ling, Experimental investigation of laterally loaded double-shear-nail connections used in midply wood shear walls, Constr. Build. Mater. 101 (2015) 761–771.
[27] JGJ/T 101-2015, Specification for Seismic Test of Buildings, Profession Standards of the People's Republic of China, Beijing, China, 2015.
[28] ISO-16670, Timber Structures-Joints made with Mechanical Fasteners-Quasi-Static Reversed-Cyclic Test Method, International Organization for Standardization (ISO), Geneva, Switzerland, 2003.
[29] ASTM: E2126-11, Standard Test Methods for Cyclic (Reversed) Load Test for Shear Resistance of Vertical Elements of the Lateral Force Resisting Systems for Buildings, ASTM Standards, West Conshohocken, PA, USA, 2012.
[30] H. Xiong, Y. Liu, Experimental study of the lateral resistance of bolted glulam timber post and beam structural systems, J. Struct. Eng. 142 (4) (2014). E4014002-1–E4014002-11.